Improved Thin-Airfoil Theory

M. F. Zedan* and K. Abu-Abdou*
King Saud University, Riyadh, Saudi Arabia

The classical thin-airfoil theory has been reconsidered with the purpose of improving its accuracy and extending its range of applicability. Two improvements were implemented. First, the effect of profile thickness on the overall aerodynamic parameters C_L and C_M has been allowed for. The usual expressions for these aerodynamic parameters are extended by new corrective terms and the closed-form nature is thus preserved. Second, a simple procedure has been developed to determine the coefficients in the series expansions of the vortex and source distributions by directly using the given profile coordinates instead of the less accurate numerically determined slopes. Over a wide range of Karman-Trefftz airfoil geometries and angles of attack with only five control points, it was found that the accuracy of the present method is substantially improved and its validity is extended to thickness ratios as high as 16%. Surprisingly, except for very limited situations, the accuracy of the method was found to be comparable to or even better than that of the Hess-Smith method using 100 panels.

I. Introduction

SINGULARITY methods are among the most widely used techniques in solving inviscid flowfields around airfoils. The basic idea is to simulate the airfoil by one or more types of continuously distributed or discrete singularities. This principle is quite old and can be traced back to Prandtl and his colleagues at Goettingen in the period 1912–1922.[1] Two approaches for applying this principle are available: the classical thin-airfoil theory and the surface singularity or panel approach. The latter is more powerful, but its computational complexity is enormous. In fact, its implementation had to await the recent development of large high-speed computers. Since then, a large number of panel methods have been developed by employing different types of singularities and following slightly different schemes in evaluating their strength.[2-6] On the other hand, the classical thin-airfoil theory is an approximate method limited to thin, slightly cambered airfoils operating at small incidence. Nevertheless, it is attractive for two main reasons: 1) it decouples the camber, thickness, and incidence effects whose contributions then simply become additive; and 2) the solution is obtained in analytic form using simple trigonometric series and can easily be performed on a programmable calculator.

In this classical thin-airfoil theory, the solution is split into two parts. The first combines the camber and incidence problems and completely ignores thickness. The thin airfoil, now represented by its camberline, is simulated by a vortex sheet. The vortex strength distribution $\gamma(x)$ is calculated by satisfying the tangency condition on the camberline using v/V_∞ induced on the chord line and the Kutta condition at the trailing edge. The second part allows for the thickness effect and ignores camber and incidence altogether. This reduces the solution of the thickness problem to that of the flow past a symmetrical airfoil at zero incidence and yields equal velocity contributions on the lower and upper sides. In the relevant literature on the subject, there is very little quantitative information about the range of applicability of the thin-airfoil theory beyond which its accuracy deteriorates. One of the few quoted limits is found in Anderson,[1] who globally states that the method gives "good" results for thickness ratios up to 12%.

In the present study, we set forth two objectives. The first is a detailed parameteric study to outline quantitatively the range of applicability of the classical thin-airfoil theory. The second objective is more ambitious and aims at improving the accuracy of the method and extending its range of applicability. This is achieved by satisfying the boundary conditions using the profile coordinates rather than the slopes in both the camber and thickness problems and by accounting for the effect of thickness on the lift and moment coefficients. The results of this extended thin-airfoil method are compared with those of the classical thin-airfoil theory and with the exact solution, over a wide range of thickness ratios, camber ratios, trailing-edge angles, and angles of attack, for a family of Karman-Trefftz airfoils. The results of the Hess-Smith panel method are also included in these comparisons.

II. Previous Work

The classical thin-airfoil theory is well documented in most aerodynamics texts;[1,5,7] therefore, it is sufficient to outline here only the main features needed to build on in subsequent sections.

With reference to Fig. 1, the tangency condition can be approximated, for small angles of attack and camber, by

$$\frac{dy}{dx} = \alpha - \frac{1}{2\pi V_\infty} \int_0^\ell \frac{\gamma(\xi)\, d\xi}{x - \xi} \tag{1}$$

where dy/dx is the slope of the camber line and γ the local vortex strength. A rigorous solution of integral equation (1) that satisfies the Kutta condition ($\gamma_{TE} = 0$) has been found to be

$$\frac{\gamma(\theta)}{2V_\infty} = A_0 \cot\frac{\theta}{2} + \sum_{i=1}^{\infty} A_i \sin i\theta \tag{2}$$

where θ is related to the dummy variable ξ by the transformation $\xi/\ell = 0.5\,(1 - \cos\theta)$. Substituting Eq. (2) into Eq. (1) and integrating, one obtains

$$\frac{dy}{dx} = \alpha - A_0 + \sum_{i=1}^{\infty} A_i \cos i\phi \tag{3}$$

where ϕ is related to x in the same way θ is related to ξ. Using simple Fourier analysis, the vortex coefficients are shown

Received Dec. 2, 1987; revision received June 13, 1988.

*Associate Professor, Mechanical Engineering Department.

to be

$$A_0 = \alpha - \frac{1}{\pi}\int_0^{\pi} \frac{dy}{dx}\, d\phi \tag{4}$$

$$A_i = \frac{2}{\pi}\int_0^{\pi} \frac{dy}{dx}\cos i\phi\, d\phi \qquad i = 1,2,\ldots \tag{5}$$

The aerodynamic coefficients are related to these vortex coefficients by

$$C_L = 2\pi\left(A_0 + \frac{A_1}{2}\right) \tag{6}$$

$$C_{M,LE} = -\frac{\pi}{2}\left(A_0 + A_1 - \frac{A_2}{2}\right) \tag{7}$$

Also, the zero-life angle α_0 is given by

$$\alpha_0 = \alpha - \left(A_0 + \frac{A_1}{2}\right) \tag{8}$$

The resultant velocity distributions along the upper (+) and lower (−) sides of the vortex sheet are given by

$$V = V_\infty \pm \gamma(x)/2 \tag{9}$$

The equations developed thus far are valid only for infinitely thin airfoils. The effect of thickness is added in the form of a velocity correction $u(x)$ to the right side of Eq. (9). Thus, the velocity on the upper and lower surfaces becomes

$$V = V_\infty + u(x) \pm \gamma(x)/2 \tag{10}$$

The velocity $u(x)$ is related to the thickness distribution $z(x)$ by

$$u(x) = \frac{V_\infty}{\pi}\int_0^{\ell} \frac{dz}{d\xi}\frac{d\xi}{x-\xi} \tag{11}$$

Representing "arbitrary" thickness profile shapes by the trigonometric series

$$\frac{dz}{dx} = B\cot\frac{\theta}{2} + B^*\tan\frac{\theta}{2} + \sum_{1=1}^{\infty} B_i \sin i\theta \tag{12}$$

Eq. (11) then yields

$$\frac{u}{V_\infty} = B - B^* - \sum_{i=1}^{\infty} B_i \cos i\theta \tag{13}$$

Once the B coefficients corresponding to a given profile are determined, u is evaluated from Eq. (13).

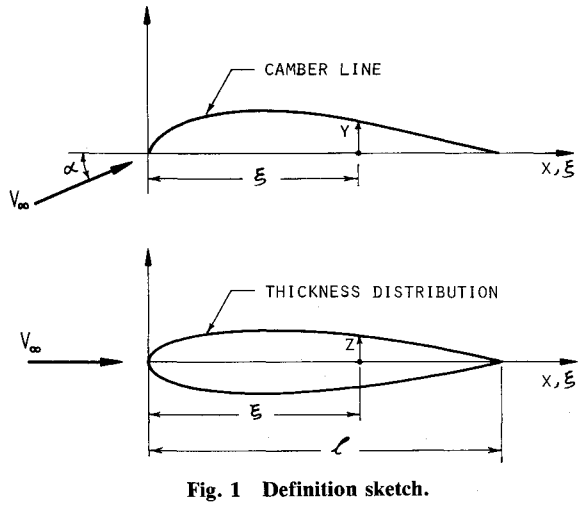

Fig. 1 Definition sketch.

III. Extended Thin-Airfoil Method

As mentioned in the introduction, two improvements are made. The first is in the numerical evaluation of the A- and B-type coefficients. The second is more fundamental and accounts for the thickness effect in determining the aerodynamic parameters.

A. Determination of the Vortex and Source Coefficients

The main advantages of the thin-airfoil theory, other than simplicity, are the closed-form expressions for various aerodynamic parameters in terms of the A- and B-type coefficients. Therefore, accurate determination of these coefficients is extremely crucial. We have found that using Eqs. (4) and (5) to determine the A-type coefficients is fairly inaccurate, if the camber line is given in tabular form and dy/dx is evaluated numerically. Numerical differentiation can introduce serious errors that will be reflected on the calculated values of the A coefficients. Instead, we integrate Eq. (3) in closed form to obtain an equation for the camber line in terms of the vortex coefficients, i.e.,

$$y(x) = \int_0^{x} \left(\frac{dy}{dx}\right) dx$$

$$y(\phi) = \frac{\ell}{2}\int_0^{\phi} \left(\frac{dy}{dx}\right)\sin\phi\, d\phi \tag{14}$$

Substituting the right side of Eq. (3) for dy/dx into the above equation and integrating, one obtains

$$y(\phi) = (\alpha - A_0)\frac{\ell}{2}(1 - \cos\phi) + A_1\frac{\ell}{4}\left(\frac{1-\cos 2\phi}{2}\right)$$

$$+ \frac{\ell}{4}\sum_{i=2}^{N} A_i\left[\frac{1-\cos(i+1)\phi}{i+1} - \frac{1-\cos(i-1)\phi}{i-1}\right] \tag{15}$$

where N is the number of Fourier coefficients retained in the γ distribution series [Eq. (2)]. Now, the $(N+1)$ coefficients $A_0, A_1, \ldots, A_N$ can be determined by satisfying Eq. (15) at $N+1$ ($= nc$) control points along the camber line and solving the resulting system of linear algebraic equations.

The B coefficients are determined from the profile thickness $z(x)$, rather than from dz/dx, in a manner similar to that used in determining the A coefficients. An equation for the profile thickness in terms of the B coefficients can be obtained by integrating Eq. (12), i.e.,

$$z(x) = \int_0^{x} \frac{dz}{dx}\, dx$$

According to Zedan and Dalton,[8] this gives

$$z(\phi) = \frac{\ell}{2}\left\{B(\phi + \sin\phi) + B^*(\phi - \sin\phi) + \frac{B_1}{2}\left(\phi - \frac{\sin 2\phi}{2}\right)\right.$$

$$\left. + \frac{1}{2}\sum_{i=2}^{M} B_i\left[\frac{\sin(i-1)\phi}{(i-1)} - \frac{\sin(i+1)\phi}{(i+1)}\right]\right\} \tag{16}$$

where M is the number of terms retained in the series of dz/dx [Eq. (12)]. The term containing the unsubscripted coefficient B accounts for rounded nose, while that containing B^* accounts for rounded tail; thus, for profiles with a cusped tail, $B^* = 0$. The B coefficients are obtained by solving a system of linear equations constructed by satisfying Eq. (16) at an appropriate number of control points ($nc = M + 2$ if tail is rounded, otherwise $nc = M + 1$).

B. Allowance for the Effect of Thickness on Aerodynamic Parameters

The lift coefficient in Eq. (6) of the classical thin-airfoil theory is obtained from the Kutta-Joukowski lift formula

$$L = \rho V_\infty \Gamma$$

with Γ being equal to

$$\int_0^\ell \gamma \mathrm{d}\xi$$

In this formulation, Γ is based on the combined camber and incidence problems only. Thus, it is implicitly assumed that the addition of the thickness velocity correction u equally on both sides of the airfoil does not contribute to Γ. Such formulation simply overlooks the fact that the contour length is generally greater on the upper surface than on the lower surface, which should add an increment to Γ. For this reason, the classical thin-airfoil theory underestimates the lift coefficient for positive incidence angles. This deficiency can be alleviated by integrating the corrected loading around the airfoil as outlined below.

Within the assumptions of the classical thin-airfoil theory, the lift coefficient can be shown to be

$$C_L = \frac{1}{\frac{1}{2}\rho V_\infty^2 \ell} \int_0^\ell \left(p_\ell - p_u\right) \mathrm{d}x \tag{17}$$

where p_ℓ and p_u are the pressures on the lower and upper surfaces of the airfoil, respectively. For ideal, incompressible flow,

$$p_\ell - p_u = \tfrac{1}{2}\rho(V_u^2 - V_\ell^2) \tag{18}$$

Substituting from Eq. (10) for V_u and V_ℓ, then

$$p_\ell - p_u = \rho(V_\infty + u)\gamma \tag{19}$$

Substituting Eq. (19) into Eq. (17) results in

$$C_L = 4 \int_0^1 \left(1 + \frac{u}{V_\infty}\right)\left(\frac{\gamma}{2V_\infty}\right) \mathrm{d}\left(\frac{x}{\ell}\right) \tag{20}$$

Finally substituting for u/V_∞ from Eq. (13) and for $\gamma/(2V_\infty)$ from Eq. (2), we get

$$C_L = 2\int_0^\pi \left(1 + B - B^* - \sum_{j=1}^M B_j \cos j\phi\right) \left(A_0 \cot\frac{\phi}{2} + \sum_{i=1}^N A_i \sin i\phi\right) \sin\phi \, \mathrm{d}\phi$$

Expanding the terms of the integrand and then integrating, one obtains, after lengthy manipulations,

$$C_L = 2\pi\left(A_0 + \frac{A_1}{2}\right)(1 + B - B^*) - \frac{\pi}{2}\left[B_1 A_2 + B_2(A_3 - A_1) + B_3(A_4 - A_2) + \ldots.\right]$$

or

$$C_L = 2\pi\left[\left(A_0 + \frac{A_1}{2}\right)\left(1 + B - B^*\right) - \frac{1}{4}\left(B_1 A_2 + \sum_{j=2}^M B_j(A_{j+1} - A_{j-1})\right)\right] \tag{21}$$

with $A_k = 0$ for $k > N$. If the thickness effect is negligible, i.e., all the B coefficients are zero, Eq. (21) reduces to Eq. (6) of the classical theory.

The same approach is used to account for the thickness effect on the moment coefficient. Taking the moment around the leading edge,

$$C_{M,\mathrm{LE}} = \frac{-1}{\frac{1}{2}\rho V_\infty^2 \ell^2} \int_0^\ell x\left(p_\ell - p_u\right) \mathrm{d}x \tag{22}$$

Substituting for $(p_\ell - p_u)$ from Eq. (19), one obtains

$$C_{M,\mathrm{LE}} = -4 \int_0^1 \left(1 + \frac{u}{V_\infty}\right) \frac{\gamma}{2V_\infty} \left(\frac{x}{\ell}\right) \mathrm{d}\left(\frac{x}{\ell}\right)$$

Substituting for $\gamma/(2V_\infty)$ and u/V_∞ from Eqs. (2) and (13), then

$$C_{M,LE} = -\int_0^\pi \left[\left(1 + B - B^* - \sum_{j=1}^M B_j \cos j\phi\right) \times \left(A_0 \cot\frac{\phi}{2} + \sum_{i=1}^N A_i \sin i\phi\right)\right](1 - \cos\phi)\sin\phi \, \mathrm{d}\phi$$

The result of the above straightforward, but lengthy, integration is

$$C_{M,\mathrm{LE}} = \frac{-C_L}{2} + \frac{1}{2}(1 + B - B^*) I_1 - \frac{1}{2} I_2 \tag{23a}$$

where I_1 and I_2 are given by

$$I_1 = \pi\left(A_0 + \frac{A_2}{2}\right) \tag{23b}$$

$$I_2 = \pi A\left(B_1 + \frac{B_2}{2}\right) + \frac{\pi}{4}\left[B_1(A_1 + A_3) + B_2 A_4 + \sum_{j=3}^M B_j(A_{j+2} - A_{j-2})\right] \tag{23c}$$

with $A_k = 0$ for $k > N$ and C_L as given by Eq. (21).

Again, if the thickness effect is negligible, Eq. (23) can be shown to reduce to

$$C_{M,\mathrm{LE}} = -\left[\frac{C_L}{4} + \frac{\pi}{4}(A_1 - A_2)\right] \tag{24}$$

which is the same equation given by Anderson[1] for the classical thin-airfoil theory.

IV. Parametric Study

The performance of the classical and the present extended thin-airfoil methods was investigated over a wide range of airfoil geometrical parameters and angles of attack. The performance was evaluated by comparing the calculated results with the exact solutions obtained by the conformal mapping technique. Results of one of most widely respected surface singularity methods (due to Hess and Smith[2]) are also included to serve as a yardstick to judge the present improvements.

The effects of airfoil thickness ratio τ, camber ratio ϵ, and trailing-edge angle β, as well as the angle of attack α, on the performance of various methods were studied by varying one of these parameters at a time while keeping the others unchanged at typical values. The typical values chosen were: $\epsilon = 4\%$, $\tau = 6\%$, $\beta = 9$ deg, and $\alpha = 6$ deg. The ranges over which these parameters were varied were: $\tau = 0$–16%, $\epsilon = 0$–10%, $\beta = 0$–13.5 deg, and $\alpha = 0$–16 deg. In order to keep the amount of computational work reasonable, the comparisons are limited to one class of airfoils—the Karman-Trefftz.

These airfoils are generated by transforming a circle according to the mapping function

$$\frac{\zeta + nc}{\zeta - nc} = \left(\frac{z + c}{z - c}\right)^n \tag{25}$$

from the complex z plane into the complex ζ plane. The resulting trailing-edge angle is uniquely determined by the exponent n according to

$$\beta = (2 - n)\pi \tag{26}$$

It can be shown that Joukowski airfoils (having a cusped trailing edge, $\beta = 0$) can be obtained using the above transformation with $n = 2$. Once n (or β) is chosen, the required ϵ and τ are obtained by properly adjusting the eccentricity of the circle in the z plane and the transformation constant c. A computer program was written to generate airfoils of this type for the chosen values of τ, ϵ, and β and compute the exact flow around them for a given α. The generated airfoil goemetry and the angle of attack α are the input to both the thin-airfoil and the Hess-Smith panel methods. Another program was written for the classical and the extended thin-airfoil methods. The program for the Hess-Smith (HS) panel method was taken from Moran[5] after modifying its input routine.

In the following results, it should be noted that the only difference between the "extended" and the "classical" thin-airfoil methods is the use of the equations developed in Sec. III.B to allow for the effect of the profile thickness on the aerodynamic parameters. The improved procedure suggested in Sec. III.A to evaluate the A and B coefficients has been implemented in the programs of both methods. The reason for including this procedure in the classical method is that it is only a refinement in the numerical scheme—not in the concept of the method.

Five control points at $x/\ell = 0.05$, 0.3, 0.65, 0.9, and 0.99 were found to be satisfactory for all the profiles investigated. The results were almost insensitive to the number of control points (which were varied between 5 and 10). However, some sensitivity to the distribution of control points was observed as their number increases. The control point at $x/\ell = 0.99$ was necessary to simulate the tails of profiles, with nonzero trailing-edge angle, by a very small rounded end. The reason for this is that the series in Eq. (16) can represent truly rounded ($B^* \neq 0$) or truly cusped ($B^* = 0$) tails only. The enforcement of this control point has been found to be more successful than expected, as manifested by the results of many test cases.

As for the HS panel method, 100 singularity elements (panels) were distributed according to a cosine law on the surface of the airfoil. In this method, adopted from Moran,[5] source and vortex distributions of uniform intensities are used over each panel. The source intensity is allowed to be different for different panels, while the vortex intensity is taken to be equal for all panels. Of course, this is a characteristic of the HS method. Other panel methods use different distributions and some use different types of singularities, viz. doublets. The source intensities over the 100 panels and the constant vortex intensity are determined by the condition of zero normal velocity at 100 control points (one at the middle of each panel) and the Kutta condition. This leads to 101 simultaneous equations compared to 5 equations in the thin-airfoil methods.

V. Results and Discussion

A. Performance for Various Thickness Ratios

Figure 2 shows the effect of τ on C_L for airfoils with $\beta = 9$ deg at $\alpha = 6$ deg. The upper part of the figure displays results for cambered airfoils with $\epsilon = 4\%$, while the lower part stands for symmetrical airfoils ($\epsilon = 0$). In both parts, the classical thin-airfoil theory, the present extended thin-airfoil method, and the HS method are compared with the exact solution. Starting with cambered airfoils, the exact C_L is seen to increase almost linearly with τ. The classical thin-airfoil theory gives a flat curve—as expected, while the present method predicts the correct rising trend with much less error. In fact, the error is less than 1.2% for $\tau \leq 8\%$ and does not exceed 4.1% at $\tau = 16\%$. These relatively small errors compare to 6.3 and 11.5% for the classical theory. The figure also indicates that the accuracy of the present method is comparable in general to that of the HS panel method. However, this method overpredicts C_L, while the HS method underpredicts C_L at most τ values. The present method gives slightly less errors for $\tau < 10\%$, while the HS method has a slight edge for $\tau > 10\%$. It should also be noted that the performance of the HS method deteriorates quite fast for thin airfoils, as indicated by the point at $\tau = 0.04$ where the error rises to around 10.6%. The results in the lower part of Fig. 2 for symmetrical airfoils show similar trends. Again, the superiority of the present method over the HS panel method becomes more evident for $\tau < 0.08$, but the opposite is correct for $\tau \geq 0.08$.

Figure 3 shows the performance results for the moment coefficient $C_{M,\mathrm{LE}}$ for the airfoils discussed in Fig. 2. Here the lower part stands for the cambered airfoils. It is obvious that the present method outperforms both the classical thin-airfoil and HS panel methods for all values of τ up to 16%. The error in C_M increases with τ to around 2.2% at $\tau = 16\%$ for the present method, compared to 4.5% for HS panel method. The results for the uncambered airfoils are shown at the top of the

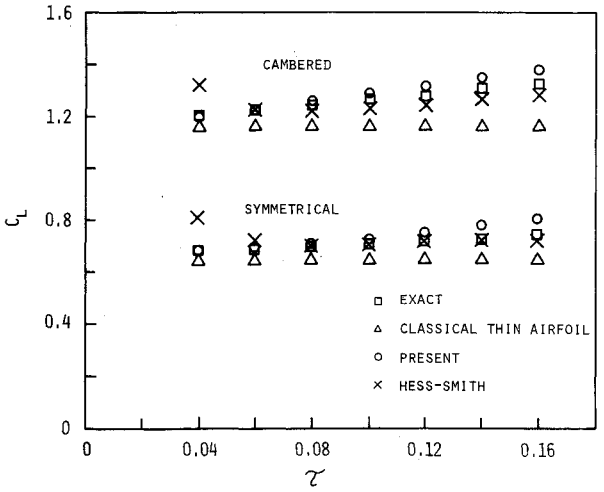

Fig. 2 Lift coefficient calculated by various methods vs thickness ratio.

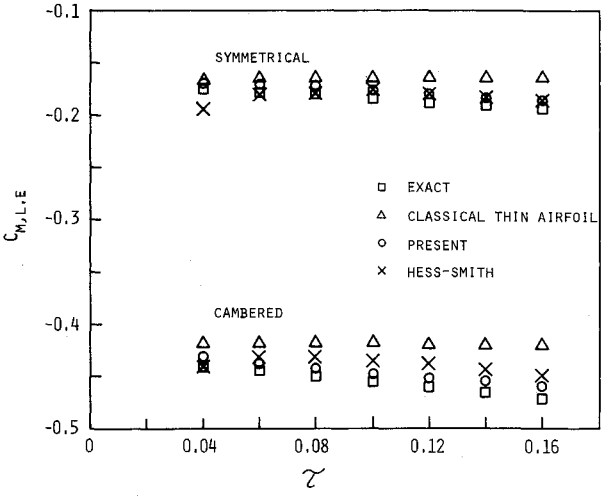

Fig. 3 Moment coefficients about leading edge vs thickness ratio.

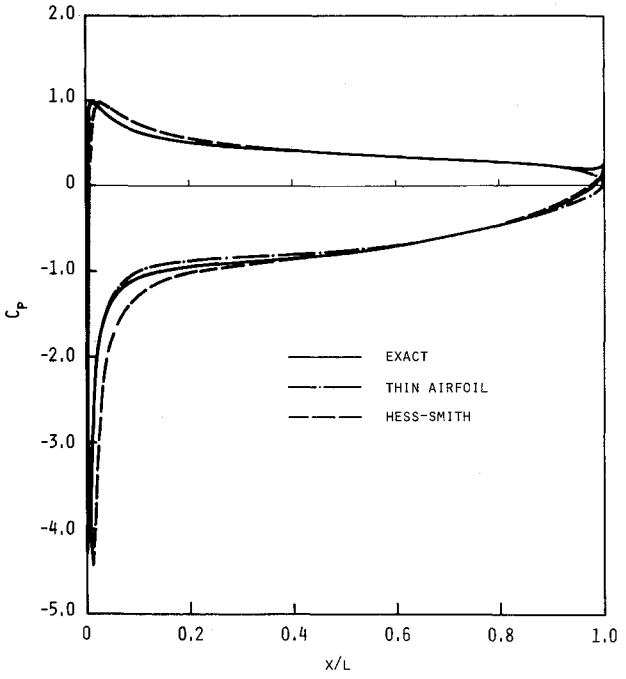

Fig. 4 Pressure distribution around a Karman-Trefftz airfoil with $\tau = 0.04$, $\epsilon = 0.04$, and $\beta = 9$ deg at $\alpha = 6$ deg.

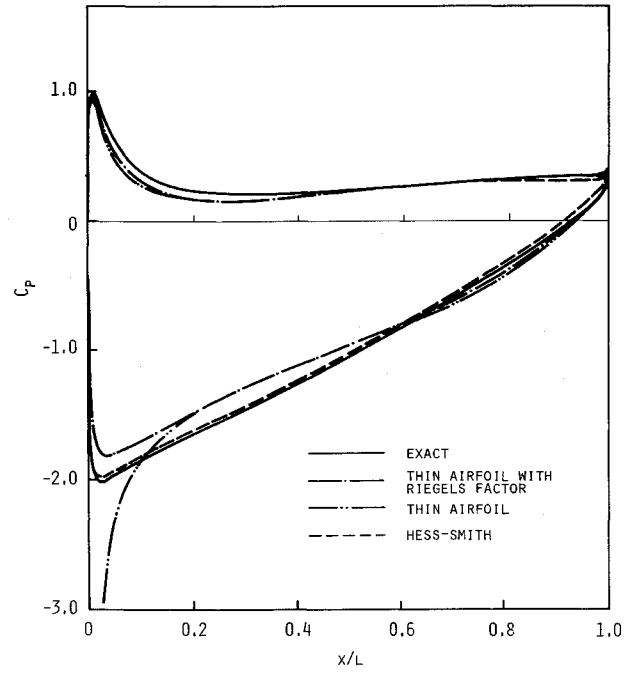

Fig. 5 Pressure distribution around a Karman-Trefftz airfoil with $\tau = 0.16$, $\epsilon = 0.04$, and $\beta = 9$ deg at $\alpha = 6$ deg.

figure. These results indicate comparable accuracy of the present and HS methods everywhere except at $\tau = 4\%$, where the latter method gives substantially greater error (10.8%). The accuracy of the classical method becomes slightly worse than in the case of cambered airfoils.

So far we have discussed the performance of various methods in terms of the overall aerodynamic parameters (C_L and C_M). As for the details of the pressure distribution, only two representative cases for $\tau = 4\%$ (thin airfoils) and $\tau = 16\%$ (thick airfoil) are shown in Figs. 4 and 5. The results for the thin-airfoil case (Fig. 4) show that the predictions of

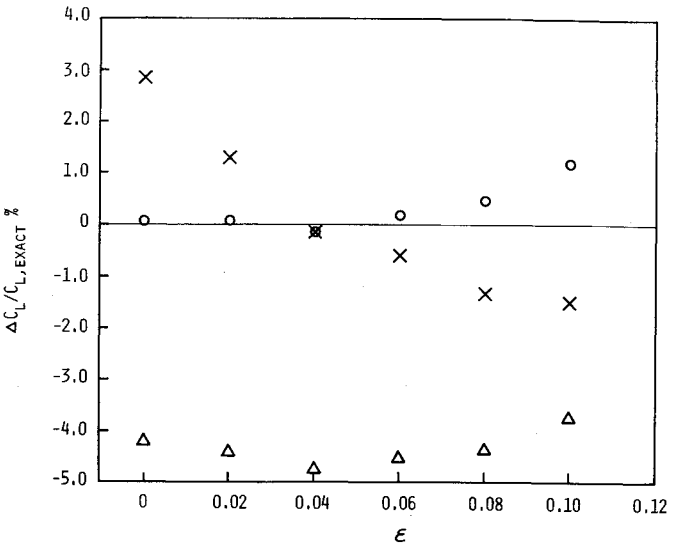

Fig. 6 Error in lift coefficient (%) vs camber ratio (symbols as in Fig. 2).

the present method agree much more closely than the HS panel method with the exact pressure distribution, except in a very small region near the tail. The small deviation of the present method in this region may be attributed to the fact that Eq. (12) cannot provide exact representation for profiles with finite trailing-edge angles. However, the approximate method suggested before to handle such profiles appears to provide reasonable accuracy.

Figure 5 shows similar results for the thickest airfoil investigated. Two curves represent the results of the present method: one with the so-called Riegels correction[7] and one without this correction. The Riegels correction is introduced by multiplying the velocity distribution in Eq. (10) by the factor $1/\sqrt{1 + (dz/dx)^2}$. This correction factor reduces the unrealistically high velocities near the leading edge and approaches unity within a short distance from the leading edge. The results of Fig. 5 with this correction appear to be more reasonable than those without it; however, both are less accurate than the HS method, especially on the suction side. However, the results were almost identical with and without Riegels correction in the case of the thin airfoil (Fig. 4). The reduced accuracy in case of thick airfoils might be attributed to the fact that the thickness effect is not strictly additive as assumed in the thin-airfoil theory. Using the root mean square of the error in C_p as a measure of the error in the pressure distribution for the cases discussed in Figs. 2 and 3, the results (not shown) indicate that the thin-airfoil method is more accurate for airfoils with $\tau \leq 0.08$, while the HS panel method is the more accurate for thicker airfoils.

B. Performance for Various Camber Ratios

The performance of the three methods was again compared for airfoils with $\tau = 6\%$, $\beta = 9$ deg, and various ϵ at $\alpha = 6$ deg. A plot of C_L vs ϵ showed an almost linear trend in the range $\epsilon = 0$–10% for all methods. The results for the present and HS methods were very close to the exact; therefore, the errors are shown in Fig. 6 instead of C_L itself. Notice that the percentage error in C_L is defined as 100 $(C_L - C_{L,\text{exact}})/C_{L,\text{exact}}$. The present method outperforms the other two methods with an error near 0.8% at $\epsilon = 0$, increasing to 1.1% at $\epsilon = 10\%$. The HS method comes next in terms of accuracy with an error of 2.9% at $\epsilon = 0$, decreasing to -1.5% at $\epsilon = 10\%$. The classical thin-airfoil method comes last with errors falling between -4.2 and -3.8%. As for the moment coefficient, Fig. 7 shows the superiority of the present method with errors ranging from -0.2 to -1.7% over the entire camber range, with the exception of the zero camber case where the error is

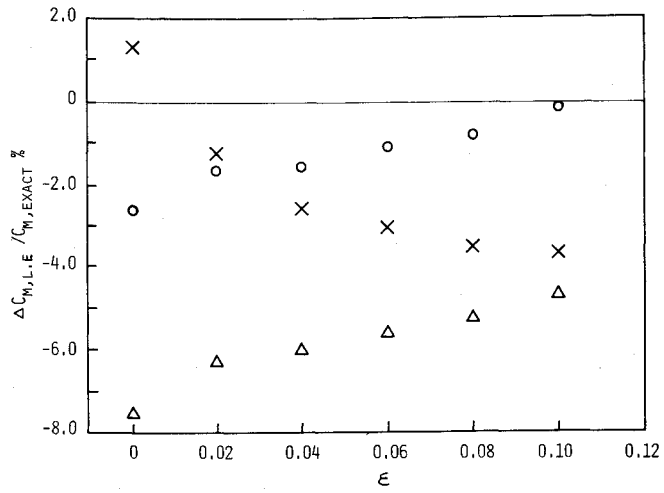

Fig. 7 Error in moment coefficient (%) vs camber ratio (symbols as in Fig. 2).

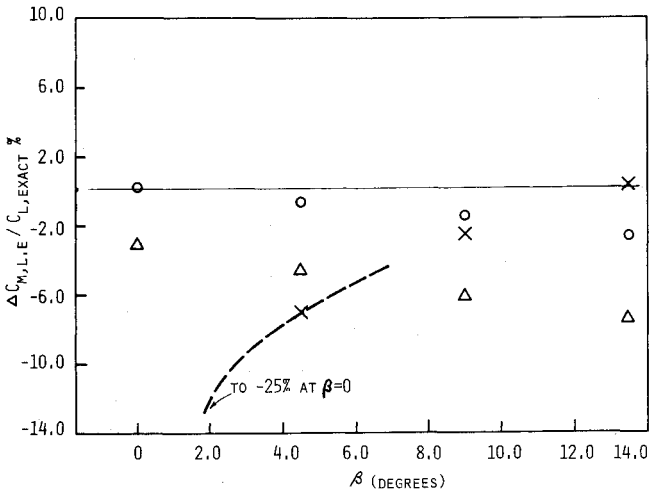

Fig. 9 Error in moment coefficient (%) vs trailing-edge angle (symbols as in Fig. 2).

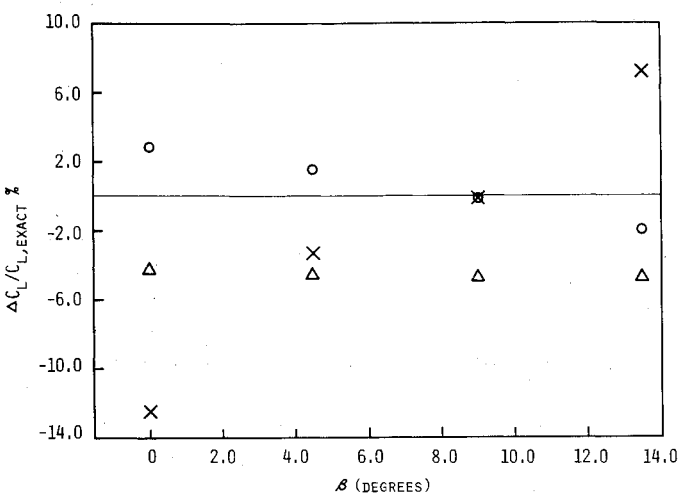

Fig. 8 Error in lift coefficient (%) vs trailing-edge angle (symbols as in Fig. 2).

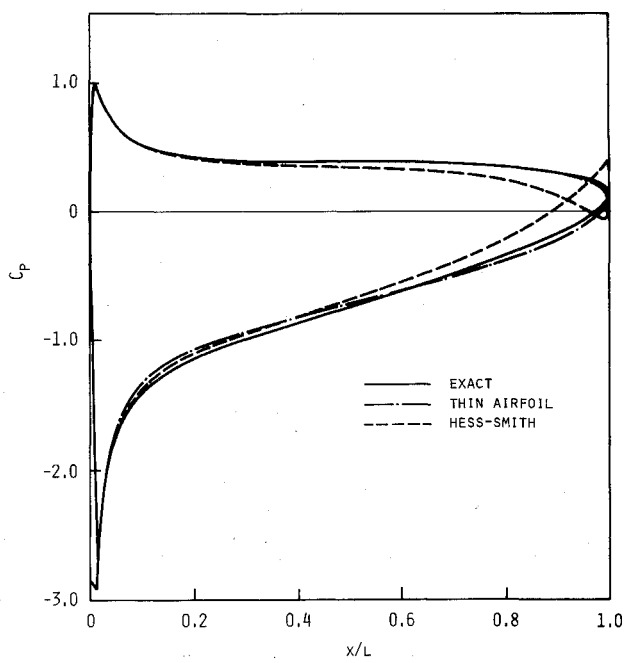

Fig. 10 Pressure distribution around Joukowski airfoil ($\beta = 0$) with $\tau = 0.06$, $\epsilon = 0.04$ at $\alpha = 6$ deg.

about -2.6%. Again, the HS panel method comes next in accuracy with errors ranging from $+1.3\%$ ($\epsilon = 0$) to -3.7% ($\epsilon = 10\%$). The classicial thin-airfoil method is the least accurate, with errors ranging between -7.5% ($\epsilon = 0$) and -4.6% ($\epsilon = 10\%$).

C. Performance for Various Trailing-Edge Angles

The performance of various methods was investigated for $\alpha = 6$ deg, $\tau = 6\%$, $\epsilon = 4\%$, and $\beta = 0$–13.5 deg. The error in the lift coefficient is shown in Fig. 8. The present method gives errors in the range 2.9% to -2%, while the classical method gives an error that is almost constant with β at a value of 4.5%. The accuracy of the HS method falls between these two methods for moderate values of β. For $\beta = 0$ the method gives an error of around -13%, while for $\beta = 13.5$ deg the error is around 7.3%. The poor performance for $\beta = 0$, which represents a Joukowski airfoil, has been recognized before by Moran[5] and recently discussed by Ardonceau,[9] while the poor performance at large values of β seems surprising. Figure 9 shows the results for the error in C_M. Again, the performance of the present method is consistently better than the other methods with errors in the range 0 to -2.5%. Surprisingly, the performances of the HS panel and the classical thin-airfoil methods are comparable, giving errors as high as 8%.

The unexpectedly large error of the HS method compared to other methods for the Joukouski airfoil case can be explained by examining the pressure distributions in Fig. 10. The results of the HS method exhibit an unrealistic loop at $x/\ell \simeq 0.90$. Ardonceau[9] found a similar behavior when the method was applied to a NACA 65012 airfoil at 10 deg incidence. He attributed the problem to the near-singular nature of the matrix for such a case, caused by the first and last elements being almost identical.

D. Performance at Various Angles of Attack

Figure 11 shows the percentage error in C_L at various angles of attack ($\alpha = 0$–16 deg) for $\tau = 6\%$, $\epsilon = 4\%$, and $\beta = 9$ deg. The present method outperforms the HS method for all values of α except at 16 deg, where the latter has a slight edge. The difference in performance is the largest at zero angle of attack, where the errors are -1 and -4.3%. The classical thin airfoil method is much less accurate than both methods at all

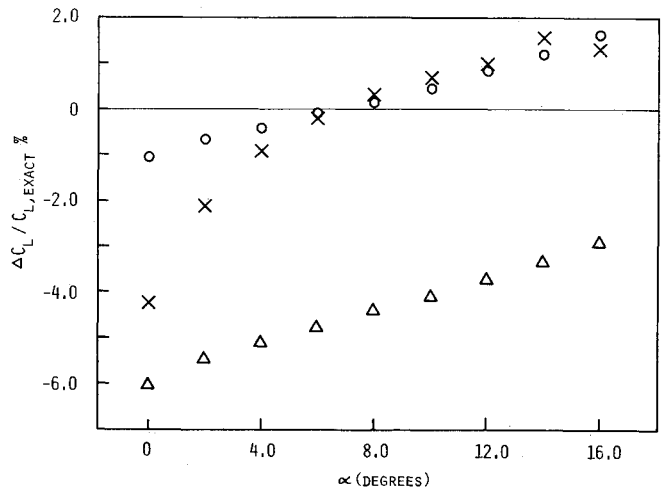

Fig. 11 Error in lift coefficient (%) vs angle of attack (symbols as in Fig. 2).

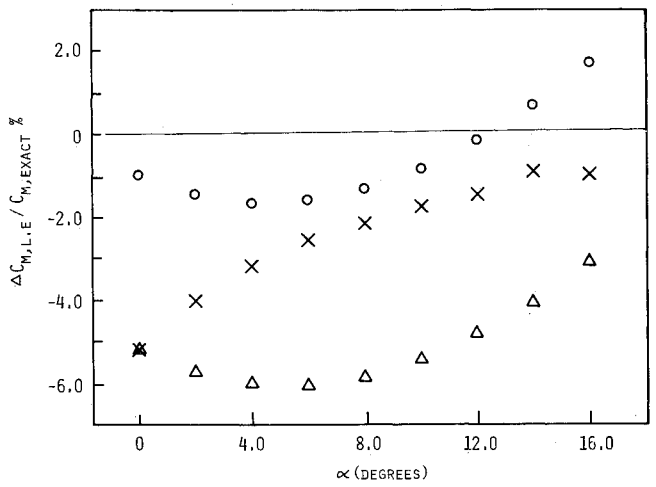

Fig. 12 Error in moment coefficient (%) vs angle of attack (symbols as in Fig. 2).

values of α with errors ranging from -2.9 to -6%. Figure 12 shows the errors in C_M vs α. The error for the present method ranges between -1.6 and 1.8%, while that of the HS panel method ranges from -0.9 to -5.2% and that of the classical thin-airfoil method from $-3.$ to -6%.

VI. Summary and Conclusions

The classicial thin-airfoil method has been extended to allow for the effect of thickness on the lift and moment coefficients. This modification did not change the simple closed-form nature of the method. Another less fundamental improvement was to satisfy the tangency condition in a form that uses the airfoil coordinates rather than the slopes. Only five control points are used to evaluate the vortex and the source intensity coefficients. This allows the method to be programmed and used on any small pocket computer or programmable calculator. Substantial improvement in the accuracy of the predicted values of C_L and C_M was obtained. The performance of this extended method was compared to that of the classical thin-airfoil method using the same number (five) of control points and to one of the highly respected panel methods due to Hess and Smith. The results of the panel method were obtained using 100 panels. These methods were used to solve the flow past a series of Karman-Trefftz airfoils. The effects of thickness ratio, camber ratio, trailing-edge angle, and angle of attack on the performance of these methods were investigated by varying one parameter at a time while keeping the others fixed at chosen nominal values ($\tau = 6\%$, $\epsilon = 4\%$, $\beta = 9$ deg, and $\alpha = 6$ deg).

The results of this study show that the performance of the extended thin-airfoil method was consistently better than the classical method, even with improved application of the tangency condition. As for the comparison with the HS panel method, the present method was more accurate in predicting C_L for thickness ratios $\tau < 8\%$, for camber ratios up to 10%, for a trailing-edge angle β up to 9 deg, and for an angle of attack α up to 14 deg, while the HS method was more accurate for $\tau > 8\%$, $\beta > 9$ deg, and $\alpha > 14$ deg. The present method was more accurate in predicting C_M for τ up to 16%, for $\epsilon > 2\%$, for β up to 9 deg, and α up to 14 deg, while the HS method was more accurate for $\epsilon = 0$, $\beta = 13.5$, and $\alpha = 16$ deg. As for the detailed pressure distribution, the thin-airfoil method with the Riegles correction—in the vicinity of the leading edge—is generally more accurate than the HS method for thin airfoils ($\tau \leq 0.08$) and for small trailing-edge angles, while the opposite is correct for $\tau > 0.08$ and for $\beta > 9$ deg.

As a final note, it should be stressed that the above conclusions are valid for the airfoil geometries and the methods investigated. Generalization beyond that should be viewed with caution. For example, other panel methods using higher-order distributions of source, vortex, and doublet elements vary in performance from the HS method. According to Moran,[5] no one panel method is considered most accurate for all profile shapes, although the HS method and doublet-based linear potential method appear to be more accurate for most moderately thick airfoils. In general, panel methods have the capability of simulating the flow past arbitrary airfoil geometries and their accuracy can be improved by extrapolation to an infinite number of panels. Clearly, the thin-airfoil theory, even with the present improvements, does not possess these powerful features.

Acknowledgment

This research has been supported by the College of Engineering Research Center, King Saud University, under Project No. 2/409.

References

[1]Anderson, J. D., "Incompressible Flow over Airfoils," *Fundamentals of Aerodynamics,* McGraw-Hill, Singapore, 1985, pp. 86-226.

[2]Hess, J. L. and Smith, A. M. O., "Calculation of Potential Flow About Arbitrary Bodies," *Progress in Aeronautical Sciences,* Vol. 8, edited by D. Kucheman, Pergamon, New York, 1967, pp. 1-138.

[3]Bristow, D. R., "Recent Improvements in Surface Singularity Methods for Flowfield Analysis about Two-Dimensional Airfoils," AIAA Paper 77-641, June 1977.

[4]Bristow, D. R., "A New Surface Singularity Method for Multi-Element Airfoil Analysis and Design," AIAA Paper 76-20, 1976.

[5]Moran, J., "Panel Method," *An Introduction to Theoretical and Computational Aerodynamics,* Wiley, New York, 1984, pp. 260-287.

[6]Maskew, B., "Prediction of Subsonic Aerodynamic Characteristics: A Case for Low-Order Panel Methods," *Journal of Aircraft,* Vol. 19, Feb. 1982, pp. 157-163.

[7]Csanady, G. T., "Thin-Airfoil Theory," *Theory of Turbomachines,* McGraw-Hill, New York, 1964, pp. 196-222.

[8]Zedan, M. F. and Dalton, C., "Higher Order Axial Singularity Distributions for Potential Flow About Bodies of Revolution," *Computer Methods in Applied Mechanics and Engineering,* Vol. 21, March 1980, pp. 295-314.

[9]Ardonceau, P. L., "Computation of the Potential Flow over Airfoils with Cusped or Thin Trailing Edges," *AIAA Journal,* Vol. 24, Aug. 1986, pp. 1375-1377.